International Journal of Materials Science ISSN 0973-4589 Volume 12, Number 2 (2017)


# Quantum Mechanical Calculations and Spectroscopic (FT-IR, FT-Raman) Investigation on 1-cyclohexyl-1-phenyl-3-(piperidin-1-yl)propan-1-ol, by density functional method

**Tintu K Kuruvilla [1], Johanan Christian Prasana[1], S. Muthu[2*], Jacob George[1]**

[1]*Department of Physics, Madras Christian College, East Tambaram 600059, Tamil Nadu, India.*

[2] *Department of Physics, Arignar Anna Govt. Arts College, Cheyyar 604407,Tamil Nadu, India.*

**E-mail: mutgee@gmail.com*

## ABSTRACT

Quantum chemical calculations such as density functional theory is a valuable research tool both in independent applications and also to conduct the verification of experimental investigations. In this work the spectroscopic studies of the title compound have been accounted using the experimental techniques and tools derived from quantum chemical calculations. 1-cyclohexyl-1-phenyl-3-(piperidin-1-yl)propan-1-ol was characterized by FT-IR and FT-Raman. The vibrational frequencies were obtained by DFT/B3LYP calculations with 6-311++G(d,p) as basis sets. The geometry of the title compound was optimised. The vibrational assignments and the calculation of Potential Energy Distribution (PED) were carried out using the Vibrational Energy Distribution Analysis (VEDA) software. In addition the NBO, first order hyperpolarizability, Molecular electrostatic potential (MEP) and HOMO LUMO energies were computed. The global reactivity indices such as electron affinity, ionization energy, chemical potential, electronegativity, hardness and softness were calculated for interpreting and predicting various aspects of chemical bonding and reaction mechanism. Fukui functions were calculated in order to explain the chemical selectivity or reactivity site in title compound. The thermodynamic properties of the title compound were calculated at different temperatures, showing the correlations between heat capacity (C), entropy (S) and enthalpy changes (H) with temperatures. The paper further explains the experimental results which are in line with the theoretical calculations and provide optimistic evidence that the title compound can be selected as a good candidate for further studies related to NLO properties.

**Keywords**: DFT; FT-IR; FT-Raman; HOMO-LUMO; NLO; Anti Parkinson agent.

## 1. Introduction

The title compound is similar to a drug which is commercially available as Trihexyphenidyl and is a member of the class of organic compounds known as aralkylamines. These are alkyl amines in which the alkyl group is substituted at one carbon atom by an aromatic hydrocarbyl group .The title compound is used as an anti cholinergic agent and anti Parkinson agent. Parkinson's disease being a major neurodegenerative disorder leads to progressive loss of nigrostriatal dopaminergic neurons. Title compound partially blocks cholinergic activity in the central nervous system, which is responsible for the symptoms of Parkinson's disease. It helps to decrease muscle stiffness, sweating, and the production of saliva which leads to better walking ability in people with Parkinson's disease. It is also known to increase the availability of dopamine, a brain chemical that is vital in the initiation and smooth control of voluntary muscle movement [1-3]. Title compound is well absorbed from the gastrointestinal tract. It disappears rapidly from the plasma and tissues, thereby eliminating its accumulation in the body during continued administration of conventional doses. Drowsiness, flushing, nausea, constipation, nervousness, blurred vision are some of its side effects. These effects lessen up as the body gets used to the medicine [4-5]. Hence the title compound is effective in reducing the rigidity of muscle spasm, tremor and excessive salivation associated with Parkinsonism. The literature review shows that no detailed quantum chemical study was carried out for the title compound. Hence, this study was carried out and the spectroscopic characterization of title compound is reported by means of IR and Raman spectra. These experimental measurements were verified with quantum chemical calculations. This has been carried out using density functional theory (B3LYP) method with 6-311++G (d,p) basis set. Properties like dipole moment, polarizability, first order hyperpolarizability, HOMO LUMO energies, molecular electrostatic potential and thermodynamic parameters have been calculated for the title compound. The natural bond orbital (NBO) analysis has been used to analyze the redistribution of electron density (ED) in various bonding and anti bonding orbitals and their respective $E^{(2)}$ energies have been calculated.

## 2. Experimental Details

The title compound was purchased from Sigma-Aldrich Chemical Company with a stated purity of 99% and was used by its very nature without further purification. The FT-IR spectrum of the title compound was recorded in the region between 4000 $cm^{-1}$ and 450 $cm^{-1}$ in SAIF IIT Chennai, India, using KBr pellet technique on Perkin Elmer Spectrum1 spectrometer. The FT-Raman spectrum for the sample was recorded in the region 4000$cm^{-1}$ to 50$cm^{-1}$ using Nd:Yag laser 1064 nm on Bruker RFS 27 spectrophotometer at SAIF, IIT Chennai, India. The observed experimental and the stimulated FT-IR and FT-Raman spectra are shown in Fig 1 and 2 respectively.

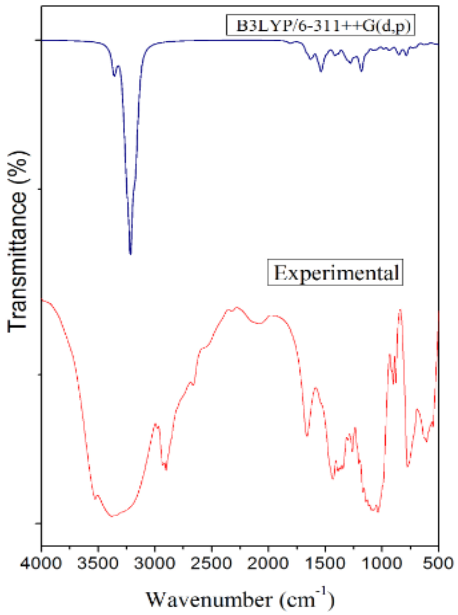


Fig 1 FT-IR spectra of 1-cyclohexyl-1-phenyl-3-(piperidin-1-yl)propan-1-ol
( Experimental and B3LYP/6-311++G(d,p))

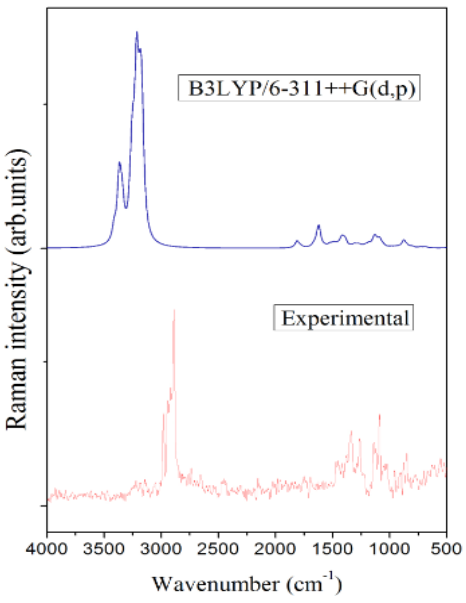


Fig 2 FT-Raman spectra of 1-cyclohexyl-1-phenyl-3-(piperidin-1-yl)propan-1-ol
(Experimental and B3LYP/6-311++G(d,p))

## 3. Computational details

The entire set of calculations was performed using the density functional theory (DFT) with 6-311++G(d, p) basis set in the Gaussian 09 program package [6]. The energy of the title compound was minimized and the intra molecular forces were brought to zero without any constraint on the geometry. This was followed by the study of the harmonic vibrational frequencies at the same level of theory for the optimized structures (opt). Scaling factor of 0.960 (above 3000 $cm^{-1}$) and 0.961 (below 3000 $cm^{-1}$) was introduced in order to fit the theoretical wavenumbers with experimental values [7]. This was done mainly to compensate for the errors arising from basis set incompleteness and neglect of vibrational anharmonicity. The symmetry considerations, the vibrational assignments and the calculation of the potential energy distribution (PED) were made with a high degree of accuracy using the Vibrational Energy Distribution Analysis (VEDA) software [8]. The GABEDIT software and ORIGIN6.1 software were used to generate the theoretical and experimental IR and RAMAN spectrum and the above were compared. The geometric structure as well as parameters, namely bond angle and bond length were obtained from CHEMCRAFT software. The first order hyperpolarisability and related properties ($\beta_{tot}$, $\alpha$, $\Delta\alpha$) of the title molecule was calculated at B3LYP level using the basis set 6-311++G(d, p). The electronic properties such as Highest Occupied Molecular Orbital (HOMO) and Lowest Unoccupied Molecular Orbital (LUMO) energies were determined. The Molecular Electrostatic Potential (MEP) was also calculated using Gauss View [9]. The Natural Bond Orbital (NBO) [10] calculations were executed in the Gaussian 09 software at the above mentioned level to understand various second order interactions taking place between the filled orbital of one subsystem and vacant orbital of another subsystem. This is a measure of intermolecular and intramolecular delocalization or hyper conjugation. The thermodynamic properties of the title compound were calculated at different temperatures, revealing the correlation between hear capacity (C), enthalpy (H) and entropy (S) with temperatures.

## 4. Results and Discussions

### 4.1 Molecular geometry

The geometrical parameters like bond length and bond angle of 1-cyclohexyl-1-phenyl-3-(piperidin-1-yl)propan-1-ol was calculated using DFT/B3LYP method with 6-311++G(d,p) basis set and some of them are listed in Table 1. The optimized molecular structure of the title compound obtained using CHEMCRAFT software is shown in Fig 3. To the best of our knowledge, exact experimental data on the geometrical parameters of title compound are not available in the literature. Therefore, it has been compared with crystal structure of similar compound [11]. It is observed that the calculated C-C bond distances are found to be similar at all levels of calculations. The molecular geometry in gas phase may differ from the solid phase owing to the extended hydrogen bonding and stacking interactions (attractive non-covalent interactions between two aromatic rings). The difference between the

theoretical and experimental geometry can mostly be attributed to the fact that calculations were performed using isolated molecule in the gaseous phase to obtain theoretical results and in solid state for experimental results. Thus, it is found that most of the optimized bond lengths and the bond angles are in reasonable agreement with the corresponding experimental values. Hence, DFT theory results in geometrical parameters which are in agreement with the experimental values.

Table 1 Optimized parameters of title compound (selected bond length ($A^0$) and bond angle ($^0$))

| PARAMETER | B3LYP/ 6-311++G(d,p) | EXPERIMENTAL* | PARAMETER | B3LYP/ 6-311++G(d,p) | EXPERIMENTAL* |
|---|---|---|---|---|---|
| BOND LENGTH ($A^0$) | | | BOND ANGLE($^0$) | | |
| C(1)-C(2) | 1.57 | 1.58 | C(2)-C(1)-O(4) | 109.9 | 109.2 |
| C(1)-O(4) | 1.438 | 1.44 | C(2)-C(1)-C(11) | 108.2 | 108.2 |
| C(1)-C(11) | 1.536 | 1.53 | C(2)-C(1)-C(17) | 112.3 | 114.7 |
| C(1)-C(17) | 1.573 | 1.58 | C(1)-C(2)-C(3) | 115.8 | 114.7 |
| C(2)-C(3) | 1.539 | 1.53 | O(4)-C(1)-C(17) | 111.8 | 111.1 |
| C(3)-N(5) | 1.465 | 1.55 | C(11)-C(1)-C(17) | 108.6 | 108.2 |
| N(5)-C(6) | 1.468 | 1.55 | C(1)-C(11)-C(12) | 120.4 | 120.4 |
| N(5)-C(10) | 1.467 | 1.55 | C(1)-C(11)-C(16) | 121.4 | 121.8 |
| C(6)-C(7) | 1.542 | 1.53 | C(1)-C(17)-C(18) | 114 | 114.7 |
| C(8)-C(9) | 1.536 | 1.53 | C(1)-C(17)-C(22) | 116.8 | 117.7 |
| C(9)-C(10) | 1.54 | 1.53 | C(2)-C(3)-N(5) | 111.3 | 111.3 |
| C(11)-C(12) | 1.401 | 1.39 | C(3)-N(5)-C(6) | 114.8 | 116.03 |
| C(12)-C(13) | 1.392 | 1.38 | C(3)-N(5)-C(10) | 114.5 | 116.03 |
| C(13)-C(14) | 1.394 | 1.38 | C(6)-C(7)-C(8) | 110.7 | 110.3 |
| C(14)-C(15) | 1.392 | 1.38 | C(7)-C(8)-C(9) | 110.7 | 110.3 |
| C(17)-C(18) | 1.55 | 1.55 | C(8)-C(9)-C(10) | 110.2 | 109.9 |
| C(17)-C(22) | 1.551 | 1.55 | C(18)-C(19)-C(20) | 111.7 | 110.3 |
| C(18)-C(19) | 1.538 | 1.53 | C(20)-C(21)-C(22) | 111.4 | 110.3 |

* Taken from Ref [11].

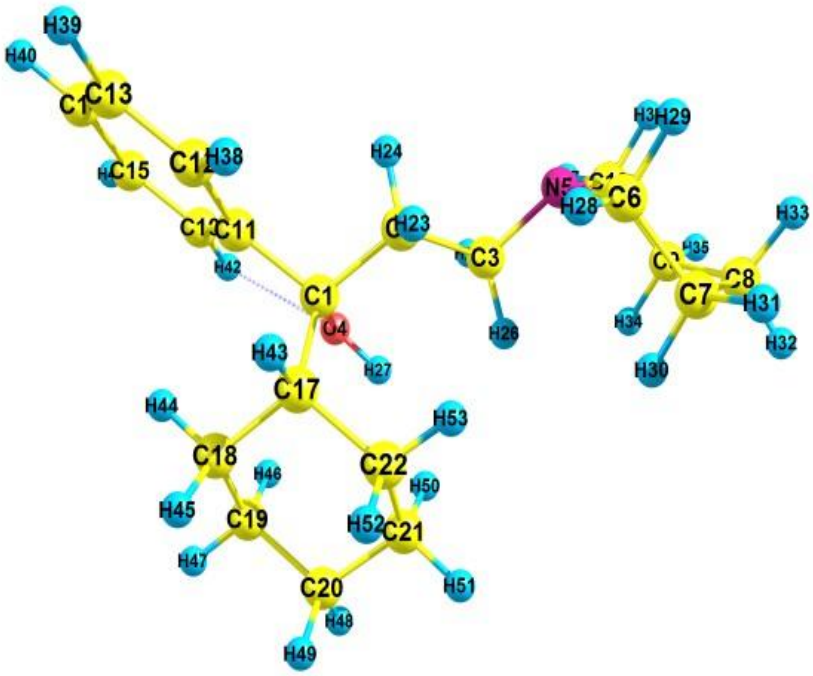


Fig 3 Optimized molecular structure of the title compound

4.2 Vibrational analysis

The IR and Raman spectra are made of variety of bands at specific wave numbers. The aim of vibrational analysis is to estimate which vibrational mode gives rise to each of these observed bands. Figs. 1 and 2 show comparative representations of theoretically predicted FT-IR and FT- Raman spectra at B3LYP/6-311++G (d, p) level of theory along with the experimental results of FT-IR and FT-Raman spectra respectively. The theoretical and experimental frequencies are presented in Table 2. The relative and absolute intensities are calculated for each of these theoretical frequencies. The theoretical values show slight deviations from the experimental ones since the theoretical wavenumbers are obtained from the isolated molecule in the gaseous phase and the experimental wavenumbers are obtained from the isolated molecule in solid state. The title compound consist of 53 atoms and has 3N-6 i.e. 153 vibrational modes. Selected vibration modes are explained in the following sections.

4.2.1 O-H Vibrations

O-H vibrations show pronounced shifts in the spectra of hydrogen bonded species. They are likely to be the most sensitive to the environment. The O-H stretching band is characterized by a broadband found near about 3600-3400 $cm^{-1}$. In the case of unsubstituted Phenol it has been shown that the frequency of OH stretching vibration in the gas phase is around 3657 $cm^{-1}$. The hydroxyl stretching vibrations generally occur in the region 3500 $cm^{-1}$ [12]. For the title compound O-H stretching vibrations obtained from B3LYP/6-311++G(d,p) were found at 3596 $cm^{-1}$ and Raman peak was found at 3560 $cm^{-1}$. PED corresponding to the stretching is 100%.

Table 2 Calculated and vibrtional wavenumbers, measured IR and Raman band positions ($cm^{-1}$) and assignments of title compound.

| Frequencies | | | | IR Intensities | | Raman Activity | | Vibrational assignments |
|---|---|---|---|---|---|---|---|---|
| Experimental | | Theorectical | | | | | | |
| IR | Raman | Unscaled | Scaled | Relative | Absolute | Relative | Absolute | |
| | 3560 (vw) | 3746 | 3596 | 30 | 29 | 76 | 22 | νOH(100) |
| | | 3216 | 3087 | 3 | 3 | 74 | 22 | νCH(97) |
| | 3047(w) | 3174 | 3047 | 31 | 30 | 51 | 15 | νCH(97) |
| 2977 | 2980(m) | 3093 | 2970 | 30 | 29 | 27 | 8 | νCH(84) |
| | 2939(s) | 3061 | 2939 | 33 | 31 | 35 | 10 | νCH(78) |
| 2930 | | 3054 | 2932 | 83 | 80 | 100 | 29 | νCH(87) |
| | 2916(vs) | 3040 | 2918 | 53 | 51 | 57 | 17 | νCH(77) |
| 2900 | 2887(vs) | 3009 | 2889 | 25 | 24 | 65 | 19 | νCH(83) |
| | 1583(w) | 1642 | 1578 | 9 | 9 | 41 | 12 | νCC(67)+βHCC(23) |
| | 1451(w) | 1512 | 1453 | 5 | 5 | 3 | 1 | βHCH(84) |
| 1430 | | 1488 | 1430 | 1 | 1 | 11 | 3 | βHCH(77) |
| 1362 | 1375(m) | 1415 | 1359 | 11 | 11 | 1 | 0 | βHCC(54) |
| 1342 | | 1392 | 1337 | 28 | 27 | 3 | 1 | βHCN(65) |
| | 1331(m) | 1385 | 1331 | 0 | 0 | 1 | 0 | βHCC(74) |
| 1297 | | 1352 | 1299 | 7 | 7 | 7 | 2 | βHCC(65) |
| 1260 | 1262(m) | 1313 | 1261 | 4 | 4 | 3 | 1 | βHCC(65) |
| 1167 | | 1212 | 1165 | 13 | 13 | 3 | 1 | βHCC(55) |
| 1140 | 1138(m) | 1183 | 1137 | 2 | 2 | 3 | 1 | δHCCC(39) |
| 1115 | | 1167 | 1121 | 1 | 1 | 2 | 1 | βHCC(52) |
| 1072 | | 1126 | 1082 | 14 | 14 | 1 | 0 | νCC(29)+βHCC(35) |
| 1034 | 1035(w) | 1075 | 1033 | 55 | 53 | 6 | 2 | νCC(39) |
| | 956(w) | 990 | 952 | 2 | 2 | 0 | 0 | νCC(38) |
| | 901(w) | 939 | 903 | 3 | 3 | 1 | 0 | δHCCC(84) |
| 899 | | 932 | 896 | 5 | 5 | 2 | 1 | νCC(52) |
| 876 | 875(w) | 906 | 871 | 15 | 14 | 2 | 1 | νCC(68) |
| | 849(w) | 874 | 840 | 3 | 3 | 1 | 0 | δHCCC(10)+βHCH(23)+νCC(10) |
| 775 | | 809 | 777 | 1 | 1 | 13 | 4 | νCC(33)+δHCCH(30) |
| | 774(w) | 804 | 773 | 2 | 2 | 2 | 1 | δHCCC(59) |
| | 698(w) | 734 | 705 | 1 | 1 | 4 | 1 | δHCCC(88) |
| | 629(w) | 650 | 624 | 11 | 11 | 1 | 0 | βHCC(82) |
| 606 | | 634 | 610 | 0 | 0 | 4 | 1 | δHCNC(50) |
| | 554(w) | 585 | 562 | 6 | 6 | 3 | 1 | βHCC(37)+δHCCC(12) |
| | 525(w) | 550 | 529 | 6 | 6 | 1 | 0 | δHCCC(42) |

Abbrevations: ν stretching, β bending and δ torsion

### 4.2.2 C-H Vibration

In aromatic compounds, the C-H stretching vibrations are expected to be found between 3100-3000 $cm^{-1}$[13]. This corresponds to the characteristic region for the identification of C-H stretching vibrations. In the present study, the bands of different intensities were observed at 2977, 2930, 2900 $cm^{-1}$ in FT-IR. Raman bands were identified at 3047, 2980, 2939, 2916, 2887 $cm^{-1}$. The theoretical values were found in the range 3087-2889 $cm^{-1}$. The above results show excellent agreement with the recorded spectral values. The PED corresponding to this vibration are found between 77-97%. The aromatic C–H in-plane bending modes of benzene and its derivatives are generally found in the region 1300–1000 $cm^{-1}$ and the C–H out-of plane bending vibrations occur in the range 1000–750 $cm^{-1}$ [14-15]. In the present study HCH bending vibration peak at 1430 $cm^{-1}$ in FT-IR and 1451, 849 $cm^{-1}$ in FT-Raman.

4.2.3 C-C Vibrations

The C-C stretching vibrations are expected to be found from 1650-1100 $cm^{-1}$. They are not influenced by the nature of substituents [16]. The theoretical bands obtained from B3LYP/6-311++G(d,p) ranges from 1578-777 $cm^{-1}$. In the present work C-C vibrations were observed at 1072, 1034, 899,876, 775 $cm^{-1}$ in FT-IR and 1538, 1035, 956, 875, 849 $cm^{-1}$ in FT-Raman. The H-C-C bending is observed in the region 1578 to 562 $cm^{-1}$. FT-IR spectra peaks at 1362, 1297, 1260, 1167, 1115, 1072 $cm^{-1}$. The Raman bands were identified at 1583, 1375, 1331, 1262, 629,554 $cm^{-1}$.

4.2.4 Other Vibrations

HCN is another type of bending vibrations which is observed in the title compound. HCN bending vibration peak at 1342 $cm^{-1}$ in FT-Raman. HCCC, HCNC and HCCH are the torsion vibrations that are found in the title compound. The occurrence of these vibrations is very less.

4.3 NBO Analysis

NBO analysis is used to study the intra and intermolecular bonding and interaction among bonds. It provides a convenient basis for investigation of charge transfer or conjugative transitions in molecular systems [17]. From the second order perturbation approach, the hyperconjugative interaction energy was deduced [18]. The stabilization energy $E^{(2)}$ for each donor NBO (i) and acceptor NBO (j) is associated with the electron delocalization between donor and acceptor, and is calculated as

$$E^{(2)} = \Delta E_{ij} = \frac{q_i(F_{ij})^2}{\varepsilon_j - \varepsilon_i}$$

where $\mathbf{q_i}$ is the donor orbital occupancy $\boldsymbol{\varepsilon_j}$ and $\boldsymbol{\varepsilon_i}$ are diagonal elements, $\mathbf{F_{ij}}$ is the off diagonal NBO Fock matrix element.

As the $E^{(2)}$ value increases, the interaction between electron donors becomes more intensive resulting in a greater extent of conjugation [19]. The intramolecular

hyperconjugative interactions of the π to π* transitions from C15-C16 π bonds to C11-C12 π* bonds leads to a stabilization energy of 20.21 kcal/mol. The title compound also has hyperconjugative interaction of σ to σ* transition from various bonds. The σ (C22-H53) to their antibonding σ* (C3-H26) leads to a stabilization energy of 100.24 kcal/mol as shown in Table 3.

Table 3 Second order perturbation theory analysis of Fock matrix in NBO basis for the title compound

| DONOR | TYPE | ED/e | ACCEPTOR | TYPE | ED/e | E(2)[a] (kcal/mol) | E(j)-E(i)[b] (a.u.) | F(i,j) (a.u.)[c] |
|---|---|---|---|---|---|---|---|---|
| C 1 - C 2 | | | C 11 - C 16 | σ* | 1.97489 | 3.16 | 1.16 | 0.054 |
| C 1 - C 2 | | | C 17 - C 18 | σ* | 1.97327 | 2.15 | 1.01 | 0.042 |
| C 2 - H 23 | σ | 1.972 | C 1 - O 4 | σ* | 1.98545 | 4.35 | 0.8 | 0.053 |
| C 2 - H 23 | | | C 3 - H 25 | σ* | 1.97512 | 2.65 | 0.92 | 0.044 |
| C 3 - H 26 | σ | 1.85949 | C 2 - H 24 | σ* | 1.97739 | 2.13 | 0.9 | 0.04 |
| C 3 - H 26 | | | C 3 - H 26 | σ* | 1.85949 | 6.14 | 1.15 | 0.075 |
| C 3 - H 26 | | | C 22 - H 52 | σ* | 1.97667 | 2.78 | 0.9 | 0.046 |
| C 3 - H 26 | | | C 22 - H 53 | σ* | 1.85921 | 98.28 | 1.18 | 0.304 |
| C 11 - C 12 | π | 1.66151 | C 1 - O 4 | σ* | 1.98545 | 5.25 | 0.55 | 0.052 |
| C 11 - C 12 | | | C 1 - C 17 | σ* | 1.96023 | 2.41 | 0.63 | 0.038 |
| C 11 - C 12 | | | C 13 - C 14 | π* | 1.66837 | 19.84 | 0.27 | 0.065 |
| C 11 - C 12 | | | C 15 - C 16 | π* | 1.98133 | 19.5 | 0.27 | 0.065 |
| C 13 - C 14 | π | 1.66837 | C 11 - C 12 | π* | 1.66151 | 18.86 | 0.28 | 0.065 |
| C 13 - C 14 | | | C 15 - C 16 | π* | 1.66056 | 19.19 | 0.27 | 0.065 |
| C 15 - C 16 | π | 1.66056 | C 11 - C 12 | π* | 1.66151 | 20.21 | 0.28 | 0.067 |
| C 15 - C 16 | | | C 13 - C 14 | π* | 1.98278 | 19.85 | 0.27 | 0.065 |
| C 15 - C 16 | | | C 18 - H 44 | σ* | 1.95967 | 2.75 | 0.7 | 0.043 |
| C 22 - H 53 | σ | 1.85921 | C 3 - N 5 | σ* | 1.97658 | 3.71 | 0.86 | 0.052 |
| C 22 - H 53 | | | C 3 - H 26 | σ* | 1.85949 | 100.24 | 1.14 | 0.302 |
| C 22 - H 53 | | | C 17 - C 18 | σ* | 1.97327 | 2.4 | 0.85 | 0.042 |

ED - Electron density.
[a]Energy of hyper conjugative interaction (stabilization energy).
[b] Energy difference between donor and acceptor i and j
[c] Fock matrix element between i and j NBO orbital.

## 4.4 Hyperpolarizability Calculations

Quantum chemical calculations are useful in the description of relationship between electronic structure of systems and its NLO response. The non-linear optical response of an isolated molecule in the electric field Ei (ω) is represented as a Taylor series expansion of total dipole moment, $\mu_{tot}$, induced by the field:

$\mu_{tot} = \mu_0 + \alpha_{ij}E_j + \beta_{ijk}E_jE_k$

where α is the linear polarizability, $\mu_0$ the permanent dipole moment and $\beta_{ijk}$ are the first hyperpolarizability tensor components [20].
The first order hyperpolarizability, is a tensor of rank 3 that can be described by a 3 x 3 x 3 matrix. Due to the Kleinman symmetry, the 27 components of 3D matrix is reduced to 10 components [21].
The total molecular dipole moment (μ), linear polarizability (α) and first-order hyperpolarizability (β) were computed at DFT level using Gaussian 09 program package and are shown in Table 4. For the study of NLO properties of molecular systems, Urea is used as one of the prototypical molecules [22]. First order hyperpolarisability of the title compound is $1.33 \times 10^{-30}$ esu which is nearly 4.43 times that of Urea. Hence the title compound is a good candidature for further studies of non linear properties.

Table 4 The dipole moments μ(D), polarizability α and the first order hyper polarizability of the title compound calculated by B3LYP/6-311++G(d,p) basis set.

| **PARAMETER** | **B3LYP/6-311++G(d,p)** | **PARAMETER** | **B3LYP/6-311++G(d,p)** |
|---|---|---|---|
| $\mu_x$ | 0.62 | $\beta_{xxx}$ | -88.70 |
| $\mu_y$ | -0.01 | $\beta_{xxy}$ | -61.54 |
| $\mu_z$ | -0.83 | $\beta_{xyy}$ | 7.73 |
| μ(D) | 1.03 | $\beta_{yyy}$ | -13.13 |
| $\alpha_{xx}$ | 288.24 | $\beta_{zxx}$ | 35.20 |
| $\alpha_{xy}$ | -7.51 | $\beta_{xyz}$ | 9.19 |
| $\alpha_{yy}$ | 255.85 | $\beta_{zyy}$ | -15.27 |
| $\alpha_{xz}$ | -11.72 | $\beta_{xzz}$ | -35.64 |
| $\alpha_{yz}$ | 3.81 | $\beta_{yzz}$ | -23.12 |
| $\alpha_{zz}$ | 182.81 | $\beta_{zzz}$ | -45.49 |
| α (a.u) | 242.30 | βtot (a.u) | 154.32 |
| α (e.s.u) | $3.59 \times 10^{-23}$ | βtot (e.s.u) | $1.33 \times 10^{-30}$ |
| Δα (a.u) | 507.93 | | |
| Δα (e.s.u) | $7.53 \times 10^{-23}$ | | |

4.5 Frontier Molecular Orbital Analysis

HOMO, Highest occupied molecular orbitals and LUMO, Lowest unoccupied molecular orbitals are the most important orbitals which take part in a chemical reaction [23]. Fig 4 shows the distribution of HOMO LUMO computed at B3LYP/6-311++G(d,p) level for title compound. The electron donating capability is characterized by the HOMO and the electron accepting capability is characterized by LUMO [24].

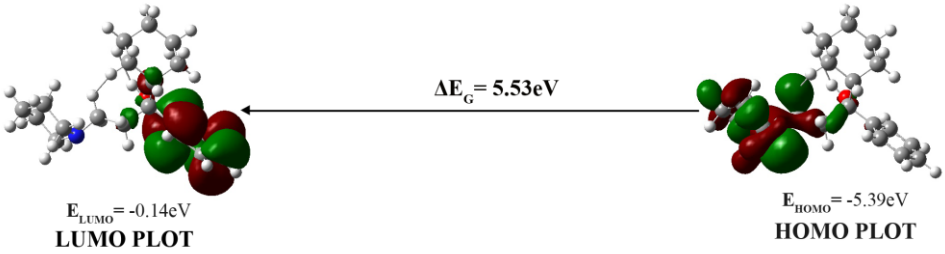


Fig 4 The atomic orbital composition of the frontier molecular orbital for the title compound.

Properties like chemical hardness of the molecules, softness, ionization potential, electron affinity and chemical potential can be determined from Frontier Optical Gap [25]. The concept of these parameters is related to each other [26] where:

Chemical potential ($\mu$) = $\frac{1}{2}(E_{LUMO} + E_{HOMO})$

Electro negativity ($\chi$) = $-\mu = -\frac{1}{2}(E_{LUMO} + E_{HOMO})$

Global hardness ($\eta$) = $\frac{1}{2}(E_{LUMO} - E_{HOMO})$

Electrophilicity = $\frac{\mu}{2\eta}$

Softness (S) = $\frac{1}{\eta}$

Table 5 Calculated energy values of title compound using B3LYP/6-311++G(d,p)

| **PARAMETERS** | **B3LYP/ 6-311++G(d,p)** |
|---|---|
| HOMO(eV) | -5.39 |
| LUMO(eV) | 0.14 |
| Ionization potential | 5.39 |
| Electron affinity | -0.14 |
| Energy gap(eV) | 5.53 |
| Electronegativity | 2.63 |
| Chemical potential | -2.63 |
| Chemical hardness | 2.77 |
| Chemical softness | 0.18 |
| Electrophilicity index | 1.25 |

The above parameters for the title compound are listed in Table 5. The IP value indicates that energy of 5.39 eV is required to remove an electron from the HOMO. The lower value of electron affinity shows higher molecular reactivity with the nucleophiles. Higher hardness and lower softness values confirm the higher molecular hardness associated with the molecule. The electrophilicity index helps in describing the biological activity of title compound.

4.6 Molecular Electrostatic Potential

Molecular electrostatic potential (MEP) are 3 dimensional diagrams that can be used to visualize charge distributions and charge related properties of the molecule. MEP for the title compound is illustrated in Fig 5. It provides visual understanding of the relative polarity of the molecule. MEP can be used to determine the electrophilic attack, nucleophilic reaction and hydrogen bonding interaction [27].

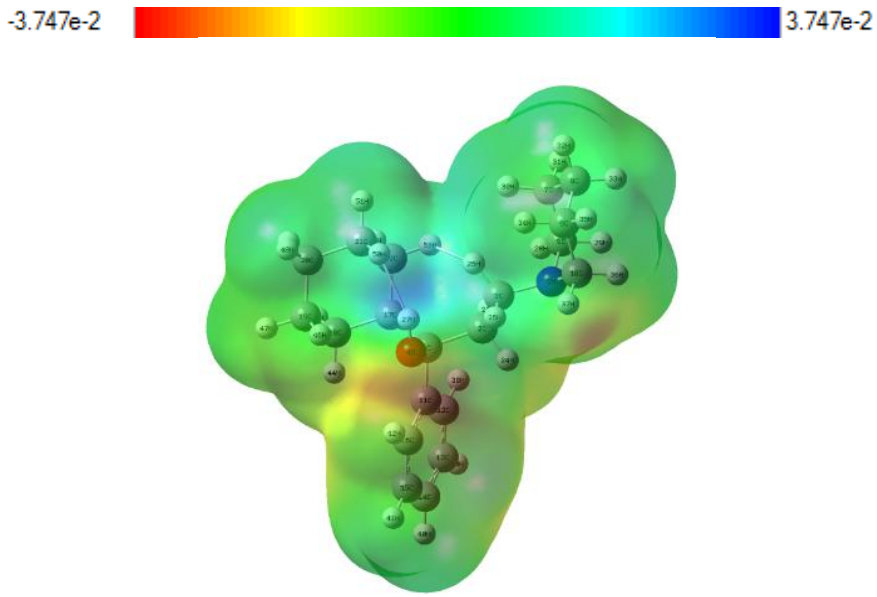


Fig 5 The total electron density surface mapped with electrostatic potential of the title compound.

MEP was calculated at the B3LYP/6-311++G(d,p) optimized geometry. The electrophilic reactivity is related to the red region of the MEP and the nucleophilic reactivity is related to the blue region. For the title compound negative regions are mainly localized over oxygen and nitrogen atoms which are most reactive sites for electrophillic attack whereas the positive regions are around hydrogen atoms which are most reactive sites for nucleophillic attack. Thus MEP is a very useful tool for giving information about intermolecular interaction.

4.7 Mulliken Population Analysis

Mulliken atomic charges play a vital role in the application of quantum mechanical calculations to molecular systems. It helps to find the charges on each atom present in the molecule. Atomic charge affects various properties like polarizability, dipole moment and electronic structure of the system [28]. The atomic charge distribution of various atoms present in the title compound was studied by Mulliken population analysis [29]. The corresponding Mulliken atomic charge values are plotted in a bar chart and are displayed in Fig 6. From the Fig, all the H atoms are positively charged

but the magnitude of charges on C atoms for the title compound were calculated to be both positive and negative. C11 atom has a positive charge of 0.117. The oxygen and nitrogen atom has large negative charge and maximum negative charge is shown by O4 atom.

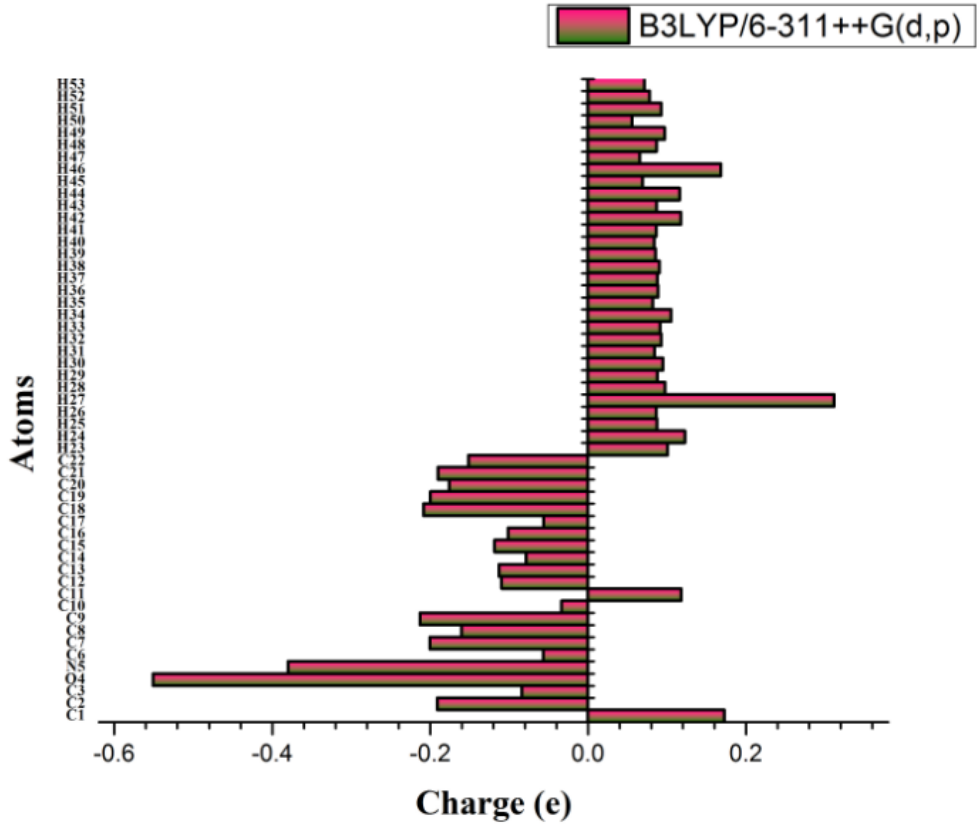


Fig 6 Mulliken population analysis of title compound.

4.8 Fukui Function

Fukui function is a commonly used basic reactivity indicator. It can be expressed as the change in density function ρ (r) of the molecule with respect to the change in the number of electrons N in the molecule, keeping the electronic potential constant. Fukui function is defined as

$F(r) = \frac{\delta\rho(r)}{\delta N}$

Where ρ(r) is the electron density, N number of electrons.

Fukui function is introduced to identify the most reactive sites for electrophillic and nucleophillic reactions within a molecule. Fukui functions can be calculated using the following equations

$f_r^- = q_{r(N)} - q_{r(N-1)}$ for electrophilic attack

$f_r^+ = q_r(N+1) - q_r(N)$ for nucleophilic attack

$f_r^0 = 1/2\,[q_r(N+1) - q_r(N-1)]$ for radical attack

In these equations, $q_r$ is the atomic charge (evaluated from Mulliken population analysis, electrostatic derived charge, etc.) at the rth atomic site is the neutral (N), anionic (N+1), cationic (N-1) chemical species [30-33].

Table 6 Condensed fukui function $f_r$ and new descriptor $(sf)_r$ for title compound.

| | **Fukui functions** | | | **local softness** | | |
|---|---|---|---|---|---|---|
| **Atoms** | $f_r^+$ | $f_r^-$ | $f_r^0$ | $s_r^+ f_r^+$ | $s_r^- f_r^-$ | $s_r^0 f_r^0$ |
| C1 | 0.004 | 0.415 | 0.210 | 0.001 | 0.087 | 0.044 |
| O4 | 0.686 | -0.775 | -0.044 | 0.143 | -0.162 | -0.009 |
| N5 | 0.681 | -0.859 | -0.089 | 0.142 | -0.180 | -0.019 |
| C6 | 0.089 | 0.510 | 0.300 | 0.019 | 0.107 | 0.063 |
| C8 | 1.358 | 0.641 | 0.999 | 0.284 | 0.134 | 0.209 |
| C10 | 0.310 | 0.258 | 0.284 | 0.065 | 0.054 | 0.059 |
| C11 | 0.925 | -0.723 | 0.101 | 0.193 | -0.151 | 0.021 |
| C13 | -0.251 | 0.415 | 0.082 | -0.053 | 0.087 | 0.017 |
| C14 | 0.203 | 0.257 | 0.230 | 0.042 | 0.054 | 0.048 |
| C16 | 0.031 | 0.179 | 0.105 | 0.006 | 0.037 | 0.022 |
| C18 | -0.046 | 0.145 | 0.050 | -0.010 | 0.030 | 0.010 |
| C20 | 0.246 | 0.635 | 0.440 | 0.051 | 0.133 | 0.092 |
| H23 | 0.143 | -0.086 | 0.029 | 0.030 | -0.018 | 0.006 |
| H24 | 0.068 | -0.194 | -0.063 | 0.014 | -0.041 | -0.013 |
| H25 | 0.069 | -0.208 | -0.070 | 0.014 | -0.043 | -0.015 |
| H26 | 1.126 | 0.164 | 0.645 | 0.235 | 0.034 | 0.135 |
| H38 | 0.043 | -0.034 | 0.004 | 0.009 | -0.007 | 0.001 |
| H50 | 0.104 | -0.064 | 0.020 | 0.022 | -0.013 | 0.004 |
| H51 | -0.407 | -0.128 | -0.267 | -0.085 | -0.027 | -0.056 |
| H52 | -0.508 | -0.247 | -0.377 | -0.106 | -0.052 | -0.079 |
| H53 | 3.303 | -0.356 | 1.473 | 0.691 | -0.075 | 0.308 |

Fukui function and local softness gives a detailed account of the reactivity and selectivity of the specific site in a molecule [34]. The local softness is related to Fukui function as follows:

$s_r^- f_r^- = Sf^-_r$ for electrophilic attack

$s_r^+ f_r^+ = Sf^+_r$ for nucleophilic attack

$s_r^0 f_r^0 = Sf^0_r$ for radical attack

Fukui functions and local softness for selected atomic sites in the title compound are listed in Table 6. It has been found that for the title compound the possible sites for nucleophillic attack is C1, O4, N5, C6, C8, C10, C11, C14, C20, H23, H24, H25,

H25, H38, H42, H50, H53. The radical attack was predicted at C1, C6, C8, C10, C11, C13, C14, C16, C18, C20, H23, H26, H38, H42, H50, H53.

4.9 Thermodynamic Properties

For the title compound, the standard thermodynamic functions: heat capacity ($C_p$), entropy (S) and enthalpy ( H), were obtained using perl script THERMO.PL [35], and are listed in Table 7. From Table 7, it can be observed that these thermodynamic functions increase with temperature in the range of 100 to 1000 K. The correlation equations between heat capacity, entropy, enthalpy changes and temperatures were expressed in the form of quadratic equations, and the corresponding fitting factors ($R^2$) for these thermodynamic properties are 0.99975, 0.9999 and 0.99975 respectively. The corresponding fit equations are as follows and the correlation graphs are shown in Fig 7.

Table 7 Thermodynamic properties of the title compound

| **T** (K) | **S** (J/mol.K) | **Cp** (J/mol.K) | **H** (kJ/mol) |
|---|---|---|---|
| 100.00 | 331.34 | 88.92 | 6.15 |
| 150.00 | 372.31 | 114.91 | 11.25 |
| 200.00 | 408.95 | 141.13 | 17.65 |
| 250.00 | 443.27 | 167.41 | 25.36 |
| 298.15 | 474.89 | 192.19 | 34.02 |
| 300.00 | 476.08 | 193.12 | 34.38 |
| 350.00 | 507.71 | 217.60 | 44.65 |
| 400.00 | 538.27 | 240.31 | 56.11 |
| 450.00 | 567.79 | 261.00 | 68.65 |
| 500.00 | 596.27 | 279.62 | 82.17 |
| 550.00 | 623.72 | 296.29 | 96.58 |
| 600.00 | 650.15 | 311.20 | 111.77 |
| 650.00 | 675.59 | 324.55 | 127.67 |

$C = 22.08356 + 0.66727T - 3.10223 \times 10^{-4} T^2 (R^2 = 0.99975)$
$S = 257.36641 + 0.79596T - 2.32947 \times 10^{-4} T^2 (R^2 = 0.9999)$
$H = -4.75399 + 0.007471T + 1.96096 \times 10^{-4} T^2 (R^2 = 0.99975)$

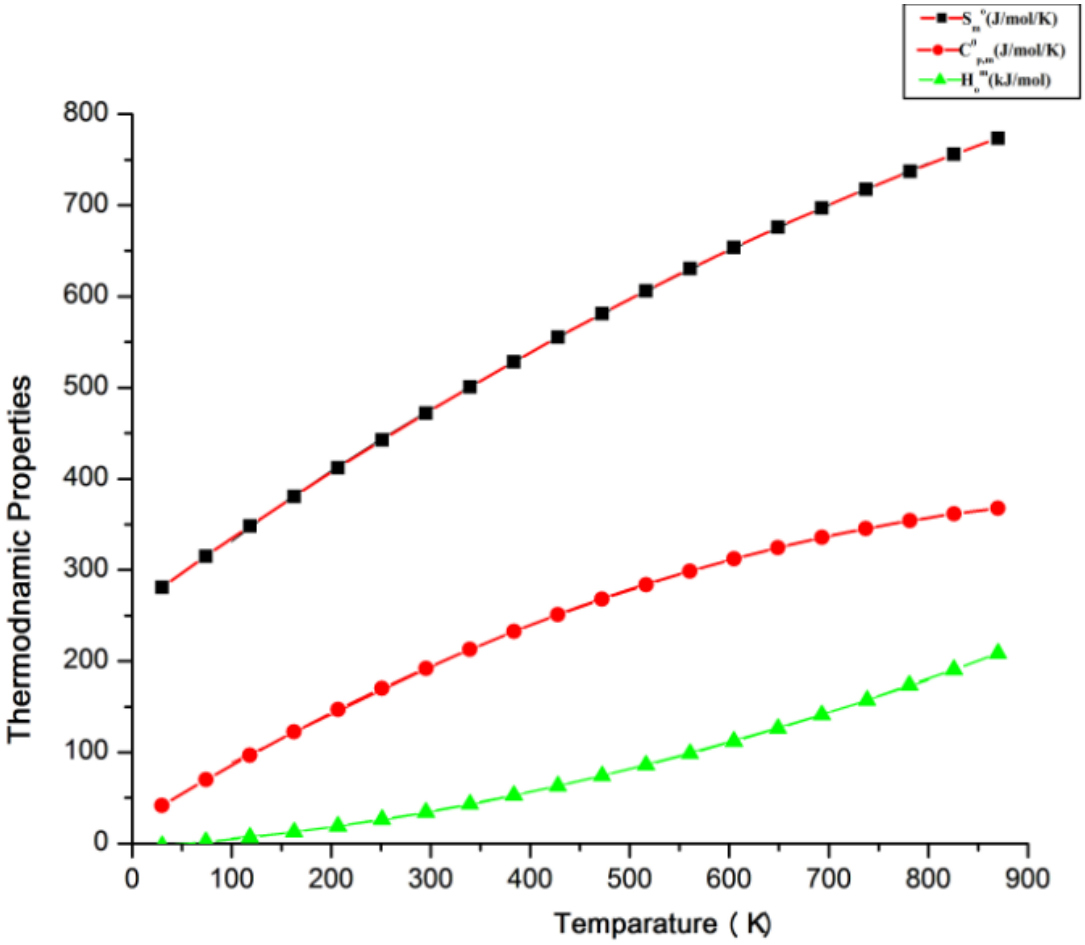


Fig 7 Correlation graphs of entropy, heat capacity and enthalpy changes of the title compound with various temperatures.

Above data can provide useful information for further study of the title compound. They can be used to compute other thermodynamic energies and can estimate directions of chemical reactions in accordance with the second law of thermodynamics in the Thermochemical field [36] .

## 5. Conclusion

B3LYP level with the 6-311++G(d,p) basis set was utilized to conduct a detailed study on the structure, geometrical parameters, vibrational analysis, NBO. NLO, HOMO LUMO energies, Molecular Electrostatic Potential, Mulliken population analysis, Fukui Function and thermodynamic parameters of the title compound. The experimental results were in line with the theoretical values. NBO analysis was done on the title compound and it showed the occurrence of intra molecular charge transfer between the bonding and antibonding orbitals. The Non-Linear Optical (NLO) properties were calculated theoretically for the title compound. It was found that the predicated first order hyperpolarizability value is greater than that of Urea which

suggest that the title compound could be used as a NLO candidate. HOMO LUMO energies, Fukui function and MEP were calculated for the title compound. The thermodynamic properties of the title compound were calculated for different temperatures, and the correlations among the properties and temperatures were obtained. This data provides useful information for further study on the title compound with relation to thermodynamic properties. Thus the comparison of theoretical and experimental data exhibit good correlation confirming the reliability of DFT employed in the study.

## 6. References

[1] Ashwin Patel, Alankar Shrivastava, Anurekha Jain and GK Singh, Method Development and Validation for estimation of Trihexyphenedyl Hydrochloride in Tablet Dosage Forms, *Asian J. Research Chem.*, 2, 2, (2009).

[2] Patel Sanjay, D. Vidyasagar, G. Development and validation of analytical method for simultaneous estimation of trihexyphenidyl hydrochloride and trifluoperazine hydrochloride in combined solid dosage form, *International Journal of Universal Pharmacy and Life Sciences,* 2,3,(2012).

[3] McInnis, M. Petursson, H**.** Trihexyphenidyl dependence, *Acta Psychiatr Scand*. Jun; 69, 65, (1984), pp. 38-42.

[4] Blumensohn, R. Razoni,G. Shalev, A. Munitz, H. Bradycardia due to trihexyphenidyl hydrochloride, *Drug Intell Clin Pharm*, 20, 10, (1986), pp. 786-787

[5] Fisch, RZ. Trihexyphenidyl abuse: therapeutic implications for negative symptoms of schizophrenia*?, Acta Psychiatr Scand.* 75,1(1987) pp. 91-94.

[6] Frisch,M.J. Trucks,G.W. Schlegel, Scuseria, G. E. Robb, M. A. Cheeseman, J. R. Scalmani, G. Barone, V. Mennucci, B. Petersson, G. A. Nakatsuji, H. Caricato, M. Li, X. Hratchian, H. P. Izmaylov, A. F. Bloino, J. Zheng, G. Sonnenberg, J. L. Hada, M. Ehara, M. Toyota, K. Fukuda, R. Hasegawa, J. Ishida, M. Nakajima, T. Honda, Y. Kitao, O. Nakai, H. Vreven, T. Montgomery, J. A. Jr., Peralta, J. E. Ogliaro, F. Bearpark, M. Heyd, J. J. Brothers, E. Kudin, K. N. Staroverov, V. N. Kobayashi, R. Normand, J. Raghavachari, K. Rendell, A. Burant, J. C. Iyengar, S. Tomasi, S. Cossi, J. M. Rega, N. Millam, J. M. Klene, M. Knox, J. E. Cross, J. B. Bakken, V. Adamo, C. Jaramillo, J. Gomperts, R. Stratmann, R. E. Yazyev, O. Austin, A. J. Cammi, R. Pomelli, C. Ochterski, J. W. Martin, R. L. Morokuma, K. Zakrzewski, V. G. Voth, G. A. Salvador, P. Dannenberg, J. J. Dapprich, S. Daniels, A. D. Farkas, Ö. Foresman, J. B. Ortiz, J. V. Cioslowski, J. and Fox, D. J. Gaussian 09 (Gaussian, Inc., Wallingford CT, 2009).

[7] Sundaraganesan, N. Illakiamani, S. Saleem, H. Wojciechowski, P.M. Michaliska, D. FT-Raman and FT-IR spectra, vibrational assignments and density functional studies of 5-bromo-2-nitropyridine, *Spectrochim. Acta A* 61, (2005), pp. 2995-3001.

[8] Jamroz, M.H. Vibrational Energy Distribution Analysis. VEDA 4 program, Warasaw, Poland, (2004).

[9] Roy Dennington, Todd Keith, John Millam, GaussView, Version 5, *Semichem Inc.*, Shawnee Mission, KS, (2009).

[10] Glendenning, E.D.Reed, A.E. Carpenter, J.E. Weinhold, NBO version 3.1,TCL,University of Wisconsin,Madison, (1998).

[11] Lise schjelderup, Per A. Groth and Arne Jorgen Aesen,(R)-(-)-1,1-Diphenyl-3-piperidinbutan-1-ol an Anticholinergic Agent. The crystal structure of (R)-(-)-1,1-Diphenyl-3-piperidinbutan-1-ol (R,R) tartrate, *Acta Chem Scand.*, 44, pp. 284-287.

[12] Bhavani, K. Renuga , S. Muthu, S. Sankara narayanan, K. Quantum mechanical study and spectroscopic (FT-IR, FT-Raman, $^{13}C$, $^{1}H$) study, first order hyperpolarizability, NBO analysis, HOMO and LUMO analysis of 2-acetoxybenzoic acid by density functional methods, *Spectrochimica Acta Part A: Molecular and Biomolecular Spectroscopy* 136 (2015), pp. 1260–1268.

[13] Swarnalatha, N. Gunasekaran, S. Muthu, S. Nagarajan, M. Molecular structure Analysis and spectroscopic characterization of 9-methoxy-2H-furo [3, 2-g] Chromen-2-one with experimental (FT-IR and FT-Raman) techniques and Quantum chemical calculations, *Spectrochim. Acta Part A* 137 (2015), pp. 721-729.

[14] Sarojini , K. Krishnan, H. Charles C. Kanakam , Muthu, S. Synthesis, structural, spectroscopic studies, NBO analysis, NLO and HOMO–LUMO of 4-methyl-N-(3-nitrophenyl)benzene sulfonamide with experimental and theoretical approaches, *Spectrochimica Acta Part A: Molecular and Biomolecular Spectroscopy,* 108, (2013), pp. 159–170.

[15] Roges, N.P.G. A Guide to the Complete Interpretation of the Infrared Spectra of Organic Structures, Wiley, New York, (1994).

[16] Sundaraganesan, N. Illakiamani, S. Meganathan, C. Joshua, B.D. Vibrational spectroscopy investigation using ab initio and density functional theory analysis on the structure of 3-aminobenzotrifluoride, *Spectrochim. Acta A* 67 (2007), pp. 214-224.

[17] Snehalatha, M. Ravikumar, C. Hubert Joe, Sekar, I. N. Jayakumar, V.S. Spectroscopic analysis and DFT calculations of a food additive Carmoisine, *Spectrochim. Acta 72A*, 654 (2009).

[18] Sidir, I. Sidir, Y.G. Kumalar, M. Tasal E. Ab initio Hartree-Fock and density functional theory investigations on the conformational stability, molecular structure and vibrational spectra of 7-acetoxy-6-(2,3-dibromopropyl)-4,8-dimethyl -coumarin molecule. *J. Mol. Struct.* 964, (2010) pp. 134–151.

[19] Muthu, S. Elamurugu Porchelvi, E. Karabacak, M. Asiri, A.M. Sushmita S. Swathi, Synthesis, structure, spectroscopic studies (FT-IR, FT-Raman and UV), normal coordinate, NBO and NLO analysis of salicyladehyde p-chlorophenylthiosemicarbazone, *Jounal of Molecular Structure* 1081 (2015) pp. 400-412.

[20] Zhang, R. Du, B. Sun, G. and Sun, Y.X. (2002) Experimental and Theoretical Studies on o-, m- and p-Chlorobenzylideneaminoantipyrines, *Spectrochimica Acta Part A*, 75, pp. 1115-1124.

[21] Kleinman, D.A. Nonlinear Dielectric Polarization in Optical Media *Phys. Rev.* 126, (1962).

[22] Muthu, S. Uma Maheswari, J. Quantum mechanical study and spectroscopic (FT-IR, FT-Raman, 13C, 1H, UV) study, first order hyperpolarizability, NBO analysis, HOMO and LUMO analysis of 4-[(4-aminobenzene) sulfonyl] aniline by ab initio HF and density functional method, *Spectrochimica Acta Part A* 92, (2012), pp. 154– 163.

[23] Muthu , S. Uma, J. Maheswari , Tom Sundius, Molecular structural, non-linear optical, second order perturbation and Fukui studies of Indole-3-Aldehyde using density functional calculations, *Spectrochimica Acta Part A: Molecular and Biomolecular Spectroscopy,* 106, (2013), pp. 299–309.

[24] Fakuri, K. Role of frontier orbitals in chemical reactions, *science* 218(1982).

[25] Uma Maheswari, J. Muthu , S. Tom Sundius, QM/MM methodology, docking and spectroscopic (FT-IR/FT-Raman, NMR, UV) and Fukui function analysis on adrenergic agonist, *Spectrochimica Acta Part A: Molecular and Biomolecular Spectroscopy,* 137, (2015), pp. 841–855.

[26] Balamurugan, N. Charanya, C. SampathKrishnan, S. Muthu, S. Molecular structure, vibrational spectra, first order hyper polarizability, NBO and HOMO–LUMO analysis of 2-amino-5-bromo-benzoic acid methyl ester, *Spectrochimica Acta Part A: Molecular and Biomolecular Spectroscopy*, 137, (2015), pp. 1374–1386.

[27] Monirah A. Al-Alshaikh, Muthu, S. Ebtehal S. Al-Abdullah, Elamurugu Porchelvi, E. Siham Lahsasni1, Ali A. El-Emam. Structural and spectroscopic characterization of *N*-[(1*E*)-(4-FLUOROPHENYL) METHYLIDENE] THIOPHENE-2-CARBOHYDRAZIDE, A potential precursor to bioactive agents, *Macedonian Journal of Chemistry and Chemical Engineering,* 35, 1, (2016).

[28] Karunanidhi, M. Balachandran, V. Narayana, B. Karnan, M. Analyses of Quantum Chemical Parameters, Fukui Functions, Magnetic Susceptibility, Hyperpolarizability, Frontier Molecular Orbitals, NBO, Vibrational and NMR Studies of 1(4- Aminophenyl) Ethanone, *International Journal of Science and Research (IJSR).*

[29] Mahalakshmi, G. Suganya, R. Balachandran, V. Determination of Structural and Vibrational Spectroscopic Properties of 4-Amino-2, 2, 6, 6-tetramethylpiperidine using FT-IR and FT-Raman Experimental Techniques and Quantum Chemical Calculations, *International Journal of Science and Research (IJSR).*

[30] Kolandaivel, P. Praveen, G. Selvarengan, P. Study of atomic and condensed atomic indices for reactive sites of molecules, J. *Chem. Sci.*, 117 (2005), pp. 591-598.

[31] Muthu, S. Isac Paulraj, E. Spectroscopic and molecular structure (monomeric and dimeric structure) investigation of 2-[(2-hydroxyphenyl) carbonyloxy]

benzoic acid by DFT method: a combined experimental and theoretical study, *J. Mol. Struct,*. 1038, (2013) pp. 145-162.

[32] Weitao Yang, Wilfried J. Mortier, The use of global and local molecular parameters for the analysis of the gas-phase basicity of amines, *J. Am. Chem. Soc*. 108, (1986), pp. 5708-5711.

[33] Sun, Y.X. Hao, Q.L. Wei, W.X. Yu, Z.X. Lu, L.D. Wang, X. Wang, Y.S. Experimental and density functional studies on 4-(3, 4-dihydroxybenzylideneamino) antipyrine, and 4-(2, 3, 4-trihydroxybenzylideneamino) antipyrine, *J. Mol. Struct. THEOCHEM* 904, (2009), pp. 74-82.

[34] Raja, M. Raj Muhamed ,R. Muthu ,S. Suresh , M. Muthu, K. Synthesis, spectroscopic (FT-IR, FT-Raman, NMR, UV-Visible), Fukui function, antimicrobial and molecular docking study of (E)-1-(3-bromobenzylidene) semicarbazide by DFT method, *Journal of Molecular Structure,* 1130, (2017), pp. 374-384.

[35] Irikura, K.K. THERMO, PL (National Institute of Standards and Technology), Gaithersburg, MD, (2002).

[36] Noureddine Issaoui, Houcine Ghalla, Muthu,S. Flakus, H.T. Brahim Oujia. Molecular structure, vibratinal spectra, AIM, HOMO-LUMO, NBO, UV, first order hyperpolarizability analysis of 3- thiophenecarboxylic acid monomer and dimer by Hartree- Fock and density functional theory, *Spectrochimica Acta Part A:Molecular and Biomolecular Spectroscopy,* 136, (2015), pp. 1227- 1242.